Colloids and Surfaces A 532 (2017) 213–221

Contents lists available at ScienceDirect

Colloids and Surfaces A

journal homepage: www.elsevier.com/locate/colsurfa

Surface enhanced plasmon effects by gold nanospheres and nanorods in Langmuir-Blodgett films

Yung-Han Wu[a], Toyoko Imae[b,c,*], Masaki Ujihara[b]

[a] Department of Materials Science and Engineering, National Taiwan University of Science and Technology, Taipei 10607, Taiwan
[b] Graduate Institute of Applied Science and Technology, National Taiwan University of Science and Technology, Taipei 10607, Taiwan
[c] Department of Chemical Engineering, National Taiwan University of Science and Technology, Taipei 10607, Taiwan

GRAPHICAL ABSTRACT

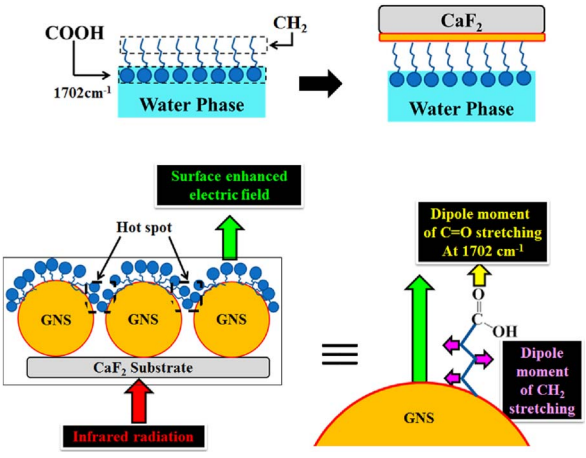

ARTICLE INFO

Keywords:
Surface enhanced infrared absorption spectrum
Gold nanosphere
Gold nanorod
Plasmon band
Langmuir-Blodgett film

ABSTRACT

Hydrophobic gold nanospheres and nanorods were synthesized by a reduction method and a seed-mediated growth method, respectively, and by the surface-modification with 1-dodecanethiol. Langmuir-Blodgett (LB) films of gold nanoparticles were prepared at different surface pressures and two-dimensional ordering of nanoparticles was evaluated. A plasmon band of nanospheres slightly red-shifted from 525 nm in water to 543 nm in chloroform but it was 634 nm at LB film. Plasmon bands at 750 and 515 nm of nanorods in water drastically changed to a band at 550 nm in chloroform but it appeared at 621 and 1000 nm. Moreover, Langmuir monolayer of eiocosanoic acid was transferred on LB films of nanospheres on CaF_2 window and transmission surface enhanced infrared absorption spectra (SEIRAS) were measured. A C═O stretching vibration band at 1702 cm^{-1} was strongly enhanced compared to other vibration bands due to the selection rule of SEIRAS. That is, the dipole moment of C═O stretching mode should be on the same direction as the surface enhanced electric field, which is perpendicular to the gold surface. From the comparison of SEIRAS for poly(amido amine) dendrimer on LB films of nanospheres and nanorods, it is apparent that the enhancement effect of nanorod LB film is higher than that of

* Corresponding author at: Graduate Institute of Applied Science and Technology, National Taiwan University of Science and Technology, Taipei 10607, Taiwan.
E-mail address: imae@mail.ntust.edu.tw (T. Imae).

http://dx.doi.org/10.1016/j.colsurfa.2017.05.015
Received 28 February 2017; Received in revised form 6 May 2017; Accepted 8 May 2017
Available online 10 May 2017

nanosphere LB film, although the surface coverage and the number density of nanorods in LB film are lower than those of nanosphere LB film, suggesting the effect of hot spots.

1. Introduction

Gold nanoparticles have been taken account some applications on industrial and biomedical fields because of their unique physical, chemical, electrical and optical properties. Thus, they have been synthesized through different techniques like laser ablation, vapor deposition electrochemical reaction and chemical reduction methods and produced with varied sizes and shapes [1–10]. At the same time, surface properties of nanoparticles were also emphasized to disperse nanoparticles in medium, and various stabilizers were loaded on the surface of gold nanoparticles. Thiol compounds are one of strongly anchoring reagents on gold surfaces and the selection of thiol compounds changes the surface characters of gold nanoparticles to be hydrophilic or hydrophobic [11–13].

The local plasmon characters of gold nanoparticles are effective for enhancing spectroscopic detection of molecules and can be applied on plasmon devices for sensing and phototherapy. The surface enhanced infrared absorption spectroscopy (SEIRS) [14–16] has been investigated as well as the surface enhanced Raman scattering [17,18] and the surface enhanced plasmon fluorescence [19–21]. On this situation, the enhancement effect depends on the situation of plasmon particles, especially, on the ordering ways of gold nanoparticles, that is, perpendicular, horizontal or random orientations of anisotropic particles [22] in addition to shapes of nanoparticles such as sphere or nonsphere. By the way, well array of gold nanoparticles has been prepared in liquid crystal matrix [23], at air-water interfaces [24], and as Langmuir-Blodgett (LB) monolayers [25–32]. However, such ordered arrays have mainly been prepared from spherical nanoparticles.

We have prepared hydrophobic gold nanorods and their well-ordered array by solvent evaporating [13] or evaporation-induced self-assembling [33]. In the present investigation, we form LB films of hydrophobic gold nanospheres and nanorods and compare their properties as a function of the surface pressure. This particle preparation method provides obvious advantages due to simple process and controllable operation parameters and ordering, and it can be applied to various nanoparticles with any shape and size. After the film preparation, the SEIRAS behaviors on LB films are discussed. Although there are reports of LB Films of gold nanorods, the rods are coated by thick silica shell [34,35]. The gold nanoparticles in the present work are coated by alkanethiol molecules and thus the shell thickness is thin but enough to protect nanoparticles from the aggregation among them and allows nanoparticles to be dispersed in organic solvents.

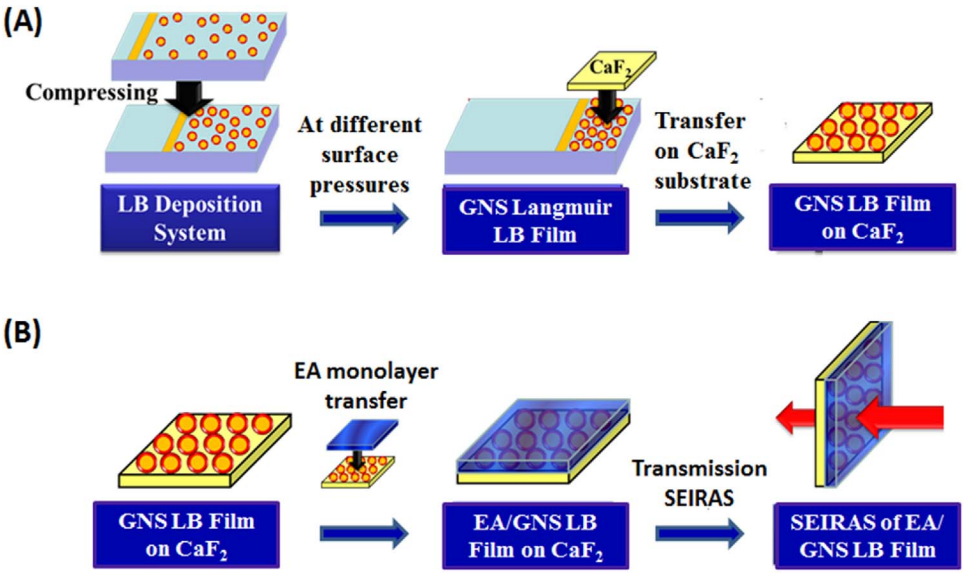

Scheme 1. Schematic illustration of preparation of (A) gold nanosphere LB films and (B) eicosanoic acid Langmuir monolayer-loaded gold nanosphere LB films.

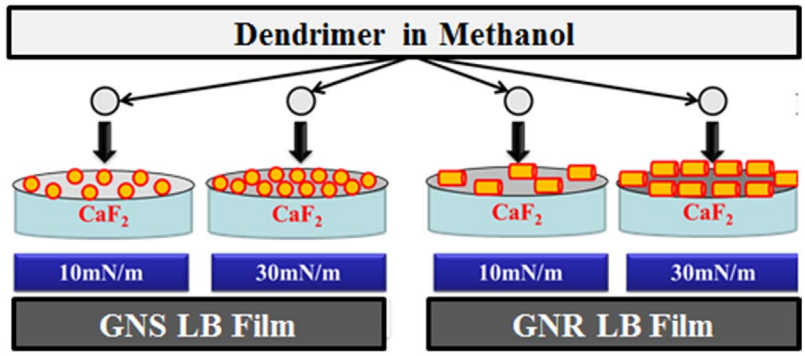

Scheme 2. Schematic illustration of preparation of PAMAM dendrimer-deposited gold nanoparticle LB films.

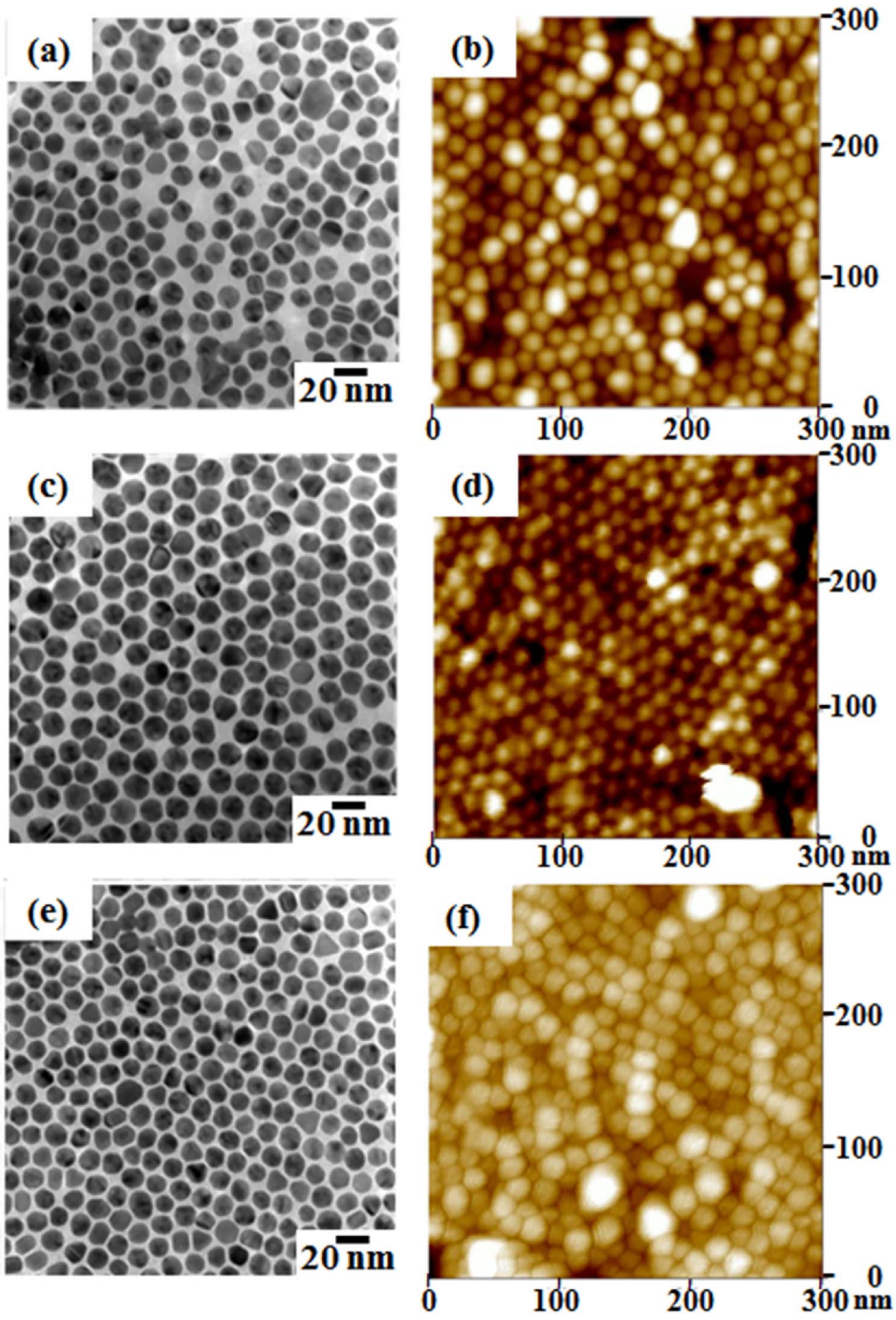

Fig. 1. TEM and AFM images of gold nanospheres in LB films. TEM: (a) (c) (e). AFM: (b) (d) (f). Surface pressure (mN/m): (a) (b) 5, (c) (d) 20, (e) (f) 40.

2. Experimental section

Citric acid (anhydrous), chloroform (99%), and hexadecyl trimethylammonium bromide (C_{16}TAB, 99%) were purchased from ACROSS Organics. Eicosanoic acid (arachidic acid) and silver nitrate were products from Wako Pure Chemical Industries, Ltd. Carboxylate-terminated generation 4.5 poly(amido amine) (PAMAM) dendrimer (ethylenediamine core, 5 wt% in methanol), sodium borohydride (98%) and sodium tetrachloroaurate(III) dehydrate (99%) were obtained from Aldrich Chemical Co. Inc. Ethyl alcohol, 1-dodecanethiol (*n*-dodecyl mercaptan) and sodium hydroxide pellets were purchased from Shimakyu's Pure Chemicals, TCI, and J. T. Baker, respectively. All chemicals were used without further purification. Ultrapure water (> 18.2 MΩ cm) was used throughout all the experiments.

LB films were prepared on a LB deposition system (Nippon laser & Electronics Lab, LB 140S-MWC). Transmission electron microscopic (TEM) images for specimens on copper grid were taken on a Hitachi H-7000 microscope. Atomic force microscopic (AFM) images were taken on a Digital Instruments NanoScope III, Veeco, for specimens on silicon wafer. Ultraviolet (UV)-visible-near infrared (NIR) absorption spectra for specimens on quartz plate or solutions in quartz cell were recorded on a JASCO V-670 spectrometer, and infrared (IR) absorption spectra for specimens on CaF_2 window were recorded on an FTIR spectrometer (Nicolet, Nexus 6700, Thermo Scientific).

Gold nanospheres were the same one, which was synthesized by the reduction of $NaAuCl_4$ and used before [36,37]: An aqueous solution (1 mM, 50 cm^3) of $NaAuCl_4$ was mixed with an aqueous solution (1 wt %, 5 cm^3) of sodium citrate (prepared from citric acid by the

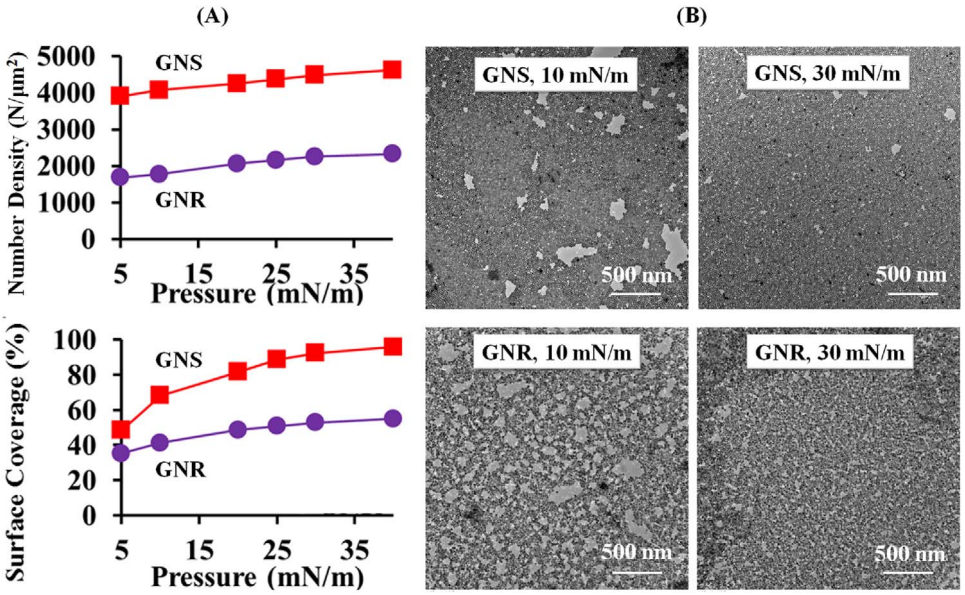

Fig. 2. (A) Number density and surface coverage of gold nanospheres (GNS) and nanorods (GNR) in LB films as a function of surface pressure and (B) TEM images of GNS and GNR at surface pressures of 10 and 30 mN/m.

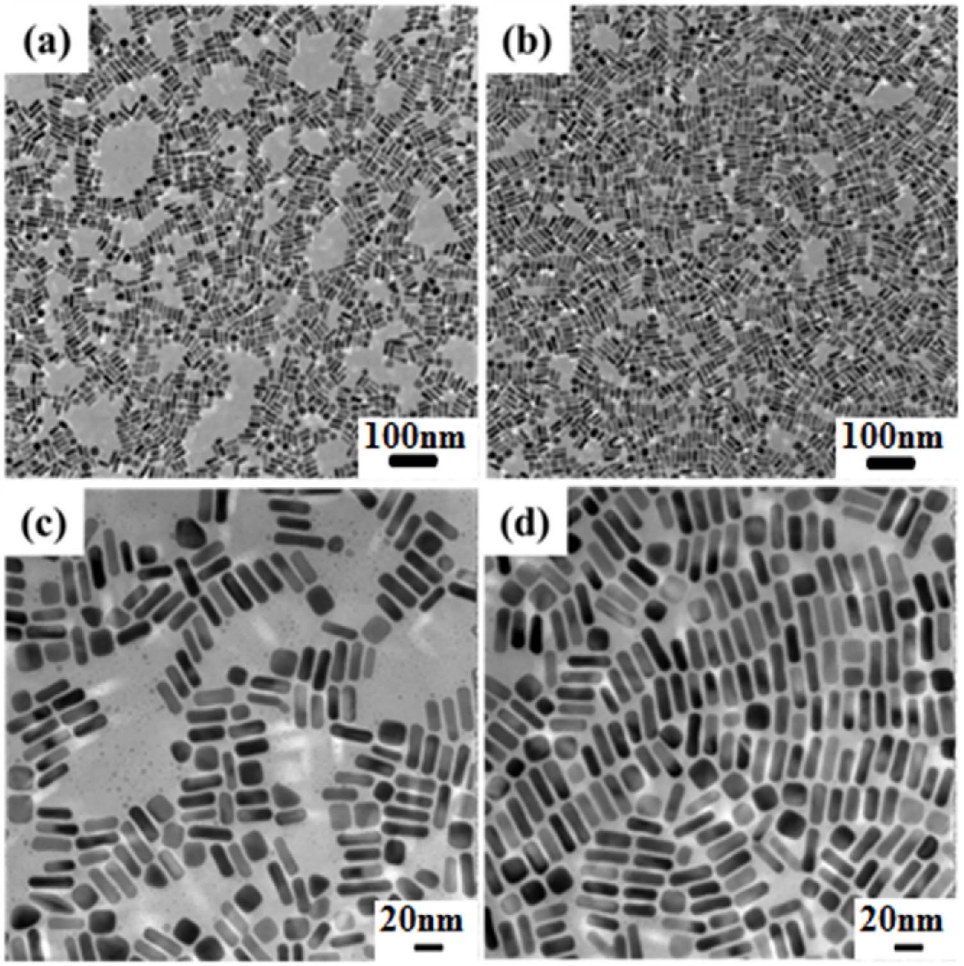

Fig. 3. TEM images of gold nanorods in LB films. Surface pressure (mN/m): (a) (c) 10, (b) (d) 30.

neutralization) and the mixture were heated at 100 °C under stirring. After a wine-red color of gold nanoparticles was ascertained, the solution was cooled down to room temperature. Then the hydrophilic surface of spherical nanoparticles was modified to be hydrophobic [12]: An aqueous solution (10 cm^3) of nanoparticles was shaken with a chloroform solution (2 mM, 10 cm^3) of 1-dodecantiol. After the transfer of the color from an aqueous solution to an organic one was affirmed, the organic phase was separated, the solvent was evaporated and the residue was solved in chloroform. The size of resultant nanospheres determined by TEM was 15 nm in average.

Gold nanorods were same as ones previously synthesized and used [37,38], which were prepared in accordance with a seed-mediated

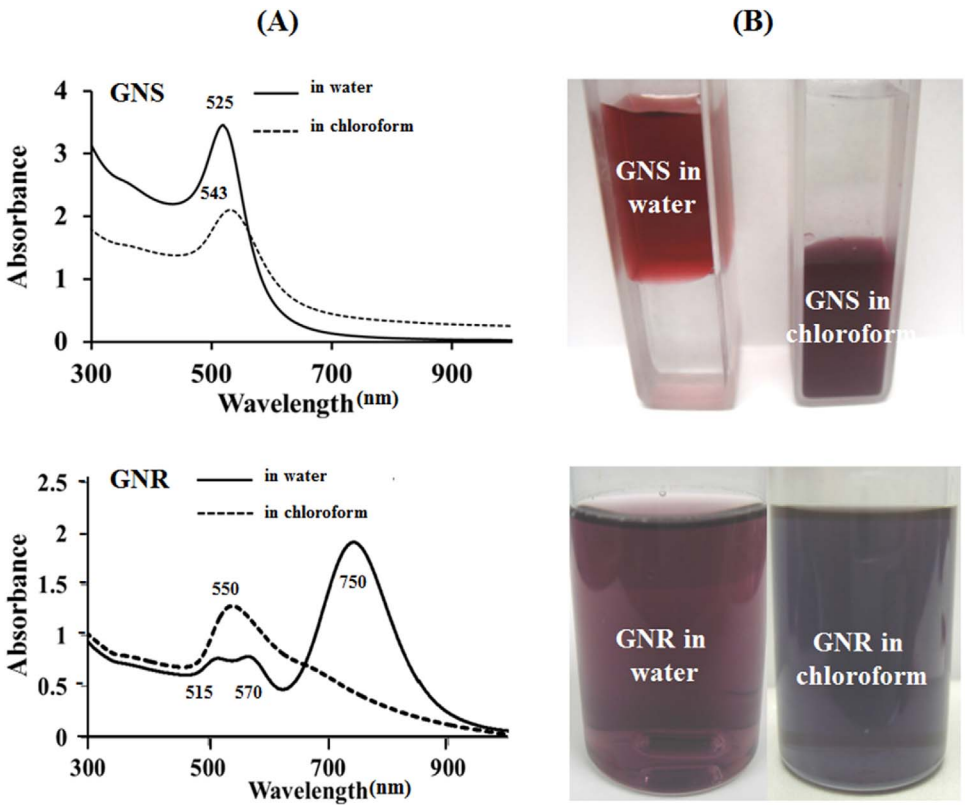

Fig. 4. (A) UV–vis-NIR absorption spectra and (B) photos of gold nanospheres (GNS) and nanorods (GNR) in water and chloroform.

method. The dispersion of produced gold nanorods was dialyzed to remove the excess C_{16}TAB, after the filtration removal of crystallized C_{16}TAB at 4 °C. The surface modification of nanorods by 1-dodecanethiol was carried out at the same procedure as for nanospheres described above. The product was the mixture of rod particles with different aspect ratios of 3.4 (20 nm length, 5.9 nm width) and 1.6 (16 nm length, 10 nm width), which existed with a ratio of 81.8 and 18.2%, respectively [32].

For the preparation of LB films, the suspension of particles in chloroform was spread on water subphase in an LB trough, and chloroform was evaporated. Langmuir monolayer of nanoparticles was compressed up to desired surface pressures at a rate of 10 mm/min and transferred by the horizontal adsorption procedure on distinct types of substrates. Loading of analytes on LB films of gold nanoparticles was carried out as follows: An aliquot (14 μl) of chloroform solution (1 mM, 10 cm^3) of eicosanoic acid was spread on water subphase of an LB trough. After the solvent was evaporated, the surface pressure was raised up to 30 mN/m and the Langmuir monolayer of eicosanoic acid was transferred on CaF_2 substrates, on which LB films of gold nanoparticles at different surface pressures were beforehand transferred. The procedures are illustrated in Scheme 1. Incidentally, Langmuir monolayer of eicosanoic acid at surface pressure of 30 mN/m is in solid state, where molecules are well ordered with a monoclinic lattice unit [39]. As a reference, a monolayer of eicosanoic acid was transferred on a bare CaF_2 substrate. Separately, an aliquot (6 μl) of a methanol solution (1.5 mM, 7.5 μl) of PAMAM dendrimer was dropped on a CaF_2 substrate, on which LB films of gold nanoparticles at 10 and 30 mN/m were beforehand transferred, as seen in Scheme 2. Then the solvent was evaporated. As a reference, an aliquot of a methanol solution of dendrimer was dropped on a bare CaF_2 substrate and the solvent was evaporated.

3. Results and discussion

LB films of gold nanospheres transferred at different surface pressures were observed by TEM. As seen in Fig. 1, particles formed domains in an LB film at low surface pressure, and the hexagonal two-dimensional array of the particles was partially formed in the domains already even at 5 mN/m. The domains took two-dimensional compact arrangements in the films with increasing surface pressure, the almost uniform monolayers were finally formed at high pressures and the almost complete hexagonal close-packed structure was achieved. Supposing the hexagonal array of nanospheres, the number density and the surface coverage could be calculated and the numerical values were plotted as a function of surface pressure in Fig. 2A. The number density almost linearly increased with the pressure, while the surface coverage increased sharply at low pressure but was converging at high pressures. Incidentally, since the edge–edge separation of about 1.3 nm between particles of 12 nm in size at highest surface pressure is close to the double chain length of 1-dodecanethiol, this distance may arise from the bilayer of the alkyl chains on neighboring particles [40]. The corresponding AFM photographs also indicated similar close pacing array of nanospheres (Fig. 1).

On the LB films of gold nanorods (see Fig. 3), rods always laid horizontally to the water surface and formed small domains consisting of parallel array of rods. The compactness increased with surface pressure [41], and rods arranged with parallel array in large area. This array is like that by self-assembling from the evaporation of solvent from a medium concentration on a substrate [13,42] but different from that in evaporation-induced self-assembling superlattice on a substrate, where gold nanorods were perpendicularly ordered on substrates [33]. The number density and the horizontal surface coverage of nanorods increased almost linearly up to 40 mN/m, as seen in Fig. 2A. Although the number density and the surface coverage increased with surface pressure for both nanospheres and nanorods, both parameters for nanospheres were always higher (almost double) than those for nanorods because of the less ability for closest packing of nanorods and the coexistence of nanorods with large and small aspect ratios (see Fig. 2B).

Characteristic difference between nanospheres and nanorods was observed on plasmon bands in UV–vis absorption spectra as compared

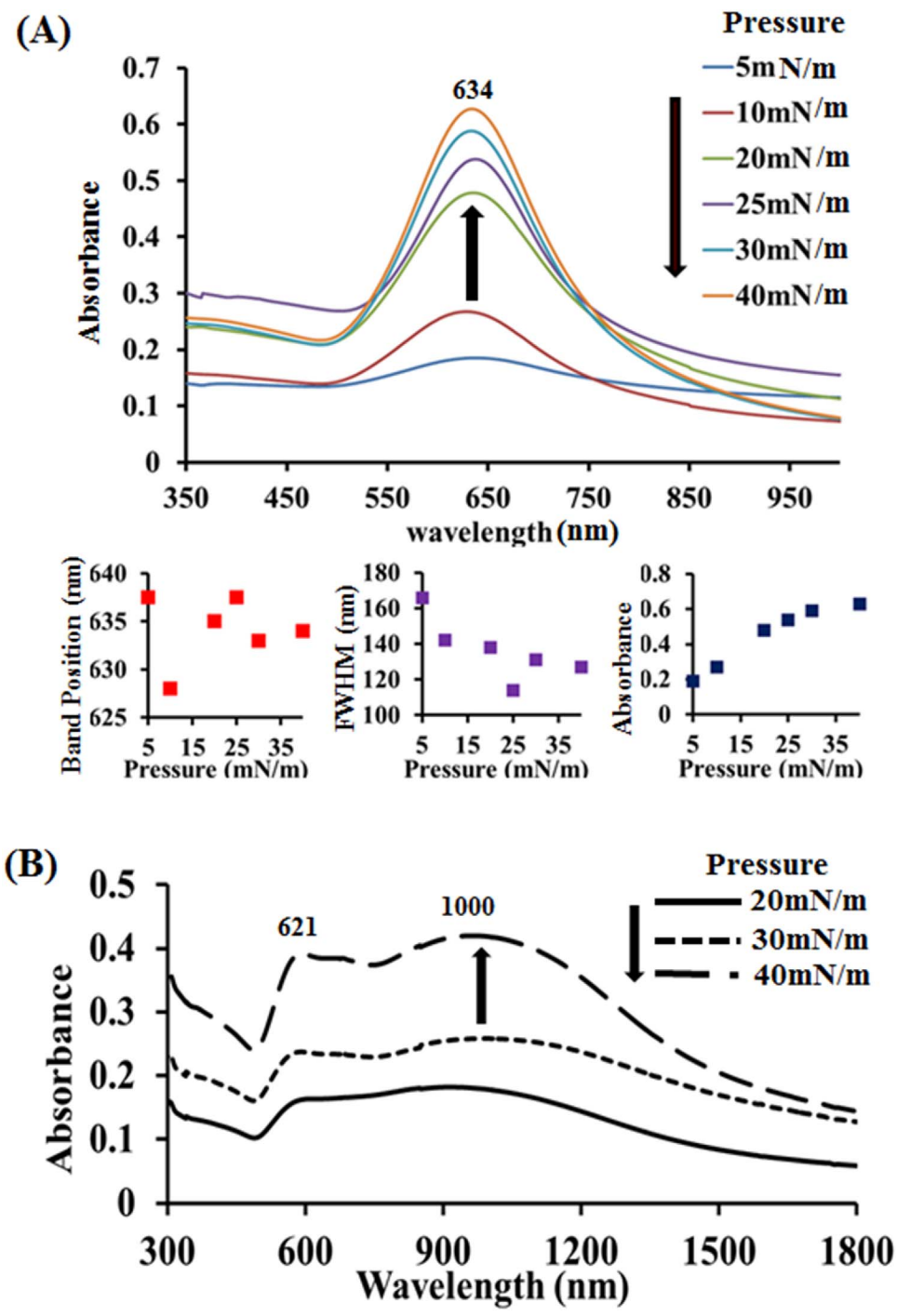

Fig. 5. UV–vis-NIR absorption spectra of gold (A) nanospheres and (B) nanorods in LB films at different surface pressures. Fig. 5(A) includes plots of band position, FWHM and absorbance as a function of surface pressure.

in Fig. 4A. Hydrophilic nanospheres in an aqueous dispersion had a sharp plasmon band at 525 nm, which is typical to spherical gold nanoparticles in water [2]. On the other hand, hydrophilic nanorods in an aqueous dispersion displayed a main band at 750 nm and weak bands at 570 and 515 nm (Fig. 4A). It was confirmed from the simulation analysis that the plasmon bands at 750 and 515 nm are attributed to rods with an aspect ratio of 3.4 and a band at 570 nm is assigned to particles at an aspect ratio of 1.6 [37,43–45]. Plasmon bands are influenced by the dielectric constant of medium [37]. In fact, plasmon bands of hydrophobic gold nanoparticles in chloroform were at 543 nm for nanospheres and at 550 nm for nanorods (see Fig. 4A). The color of dispersion changed red to blue depending on the wavelengths of plasmon bands, as seen in Fig. 4B.

UV–vis-NIR absorption spectra of LB films of gold nanoparticles prepared at different surface pressures are shown in Fig. 5. Spectra of LB films of nanospheres displayed only one broad plasmon band at around 634 nm, which was red-shifted from a plasmon band in media (Fig. 5A) [46]. Despite of the less variation of band position, its full width at half maximum (FWHM) decreased slightly and the absorbance increased and approached to the convergence with increasing surface pressure. Meanwhile, the spectra of LB films of nanorods were characterized by two broad bands at 621 and around 1000 nm (Fig. 5B), while a strong plasmon band around 1000 nm is comparable to that observed for confeito-like gold nanoparticles [8]. The absorbance of both bands of nanorods was similar each other and increased with surface pressure as expected [47]. These tendencies of plasmon bands depending on surface pressure may relate to the increase of surface coverage and number density of nanoparticles (Fig. 2A). The increased

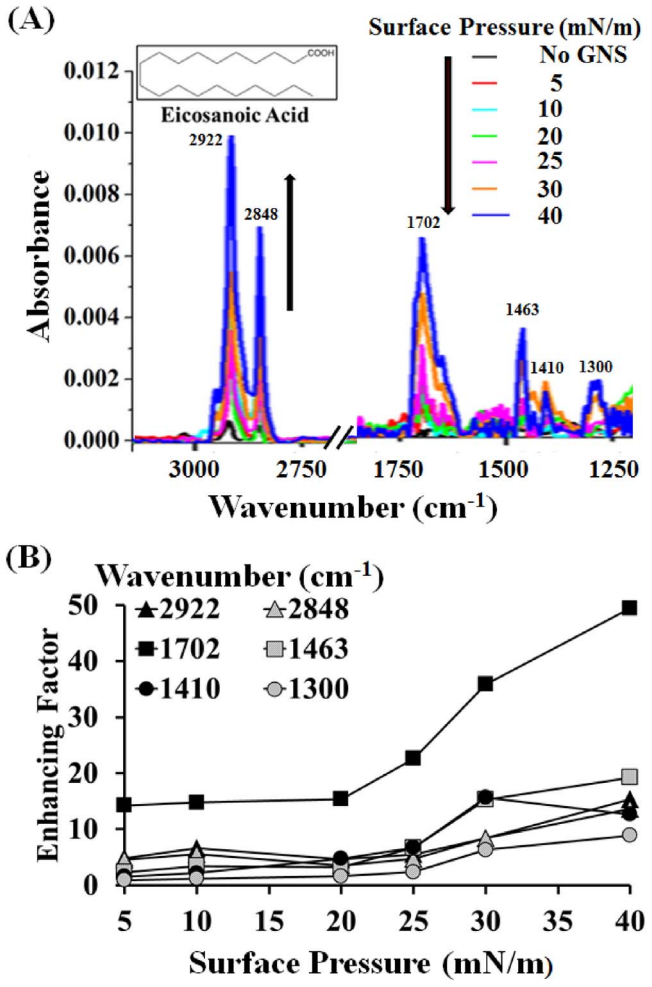

Fig. 6. (A) SEIRAS of eicosanoic acid on gold nanosphere LB films at different surface pressures. (B) Enhancement factor at different absorption bands as a function of surface pressure.

absorbance of plasmon bands is the result of the close packing of nanoparticles.

The surface enhancement effect by plasmonic gold nanoparticles was examined by transmission IR absorption spectra. IR absorption spectra of eicosanoic acid on LB films of gold nanospheres were indicative of characteristic bands at 2922, 2848, 1702, 1463, 1410, and 1300 cm^{-1}, which are assigned to CH_2 antisymmetric and symmetric stretching, C═O stretching, C—O stretching + OH bending and CH_2 bending (Scissoring and wagging) vibration modes (see Fig. 6A). When the absorbance of C═O stretching band at 1702 cm^{-1} was evaluated against an absorbance of eicosanoic acid on a substrate without LB film of nanospheres, the enhancement factor was remarkably increased at surface pressure higher than 20 mN/m (Fig. 6B). Although the similar tendency was observed even for different IR absorption bands, the enhancement factor was low. Thus, the highest enhancement factor of 50 was obtained on an IR band at 1070 cm^{-1} for LB film at 40 mN/m. This may indicate that the C═O stretching vibration dipole moment is affected by the selection rule of the surface enhancement effect [14,15], if it is perpendicularly oriented on gold surface with same direction as the surface enhanced electric field, as seen in Scheme 3.

The enhancement in IR spectra was also examined for carboxylate-terminated PAMAM dendrimer on LB films of gold nanoparticles at 10 and 30 mN/m. Characteristic IR bands of dendrimer were observed at 1635, 1560 and 1396 cm^{-1}, which can be attributed to amide I, amide II + COO• antisymmetric stretching and COO• symmetric stretching vibration modes, respectively (Fig. 7). The absorbance increase of IR bands on LB film against a corresponding band of dendrimer on substrate without LB film of gold nanoparticles are listed in Table 1, which includes numerical values of the surface coverage and the number density. The relative absorbance increased more than two times at high surface pressure, similar to the increase of the surface coverage and the number density. This means that the enhancing effect depends on the plasmon electric field intensity, which is adjustable by the number density occurring with the increase of the surface pressure. It is also apparent from Table 1 that the increase of relative absorbance of IR bands at 1396 and 1635 cm^{-1} was almost similar between nanospheres and nanorods, but a band at 1560 cm^{-1} was intensified about twofold

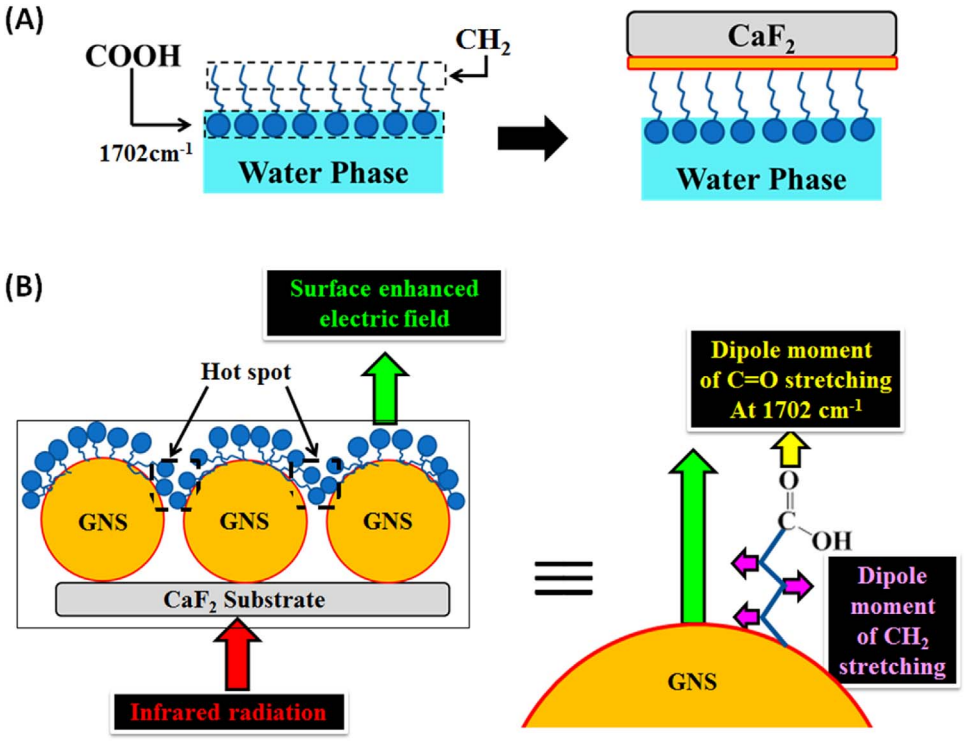

Scheme 3. Schematic illustration of (A) horizontal transfer of eicosanoic acid Langmuir monolayer on gold nanosphere LB film on CaF_2 substrate and (B) mechanism of surface enhancement effect on gold nanoparticles.

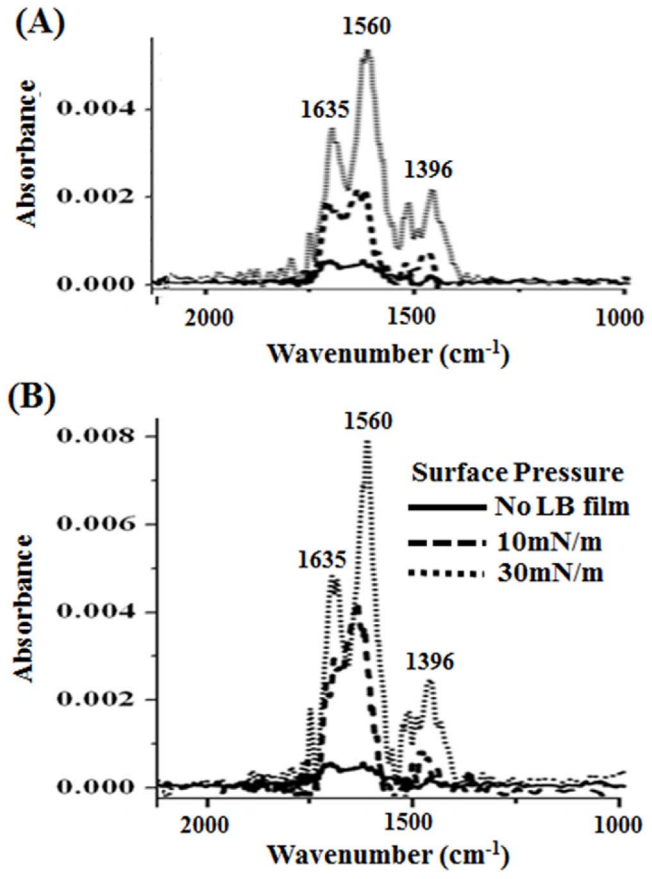

Fig. 7. SEIRAS of PAMAM dendrimer on LB films of gold (A) nanospheres and (B) nanorods at surface pressures of 10 and 30 mN/m. FTIR spectra on substrate without LB films are also included.

Table 1
Characterization of LB films of gold nanoparticles.

Particle	sphere		rod	
Surface pressure (mN/m)	10	30	10	30
Enhancement factor at 1635 cm^{-1}	3.8	7.1	5.7	9.7
Enhancement factor at 1560 cm^{-1}	4.5	11.7	9.0	17.0
Enhancement factor at 1396 cm^{-1}	3.1	11.5	3.1	12.9
Surface coverage (%)	68	92	41	53
Number density (N/μm^2)	4080	4480	770	2260

for nanorods more than for nanospheres, although the surface coverage and the number density of nanorods were about half in comparison with those of nanospheres. This indicates the stronger enhancement effect of nanorods, maybe, coming from the stronger hot spot effects [18,48], raising from the close parallel arrangement of rods as seen in TEM images. In addition, the C═O vibration dipole of COO• group should be oriented to the same direction as the plasmon electric field similar to C═O in eicosanoic acid (see Scheme 3).

4. Conclusions

The films of nanoparticles used in this study were prepared through three steps consisting of synthesis, surface modification and film forming of nanoparticles. Gold nanospheres and nanorods synthesized by chemical procedure were surface-modified to be hydrophobic. Hydrophobic nanoparticles formed Langmuir monolayers on water subphase in LB deposition trough, and their surface coverage (or density) and arrangement uniformity depended on the surface pressure. Moreover, the film formation raised red-shift of a plasmon band of nanorods to be close to 1000 nm.

The SEIRAS effect of nanoparticle LB films was examined by means of eicosanoic acid and PAMAM dendrimer as analytes, which have carboxylic acid head group or carboxylate periphery group, respectively. It was confirmed that the films with high coverage and particle density provided larger enhancement factors, the enhancement effect of nanorods was superior to that of nanospheres, and the SEIRAS selection rule for the orientation of carboxyl acid and carboxylate occurred on gold nanoparticles.

Thus, although the surface enhancement factor of LB films of gold nanoparticles is not necessarily high in comparison with previous reports [16], the characteristic plasmon band at NIR region (1000 nm) and the surface enhancement effect of a specific IR band based on selection rule give us the expectation towards the utilization as photosensitizers and chemo- and biosensors of nanoparticles obtained in the present work.

Acknowledgements

We acknoweledge to Prof. Jinn P. Chu and Prof. Fu Han Ho for their adequate guidance and helpful suggestion.

References

[1] F. Mafuné, J. Kohno, Y. Takeda, T. Kondow, H. Sawabe, Formation of gold nanoparticles by laser ablation in aqueous solution of surfactant, J. Phys. Chem. B 105 (2001) 5114–5120, http://dx.doi.org/10.1021/jp0037091.
[2] A. Manna, T. Imae, K. Aoi, M. Okada, T. Yogo, Synthesis of dendrimer-passivated noble metal nanoparticles in a polar medium: comparison of size between silver and gold particles, Chem. Mater. 13 (2001) 1674–1681, http://dx.doi.org/10.1021/cm000416b.
[3] A. Manna, T. Imae, T. Yogo, K. Aoi, M. Okazaki, Synthesis of gold nanoparticles in a winsor II type microemulsion and their characterization, J. Colloid Interface Sci. 256 (2002) 297–303, http://dx.doi.org/10.1006/jcis.2002.8691.
[4] Y. Lu, G.L. Liu, J. Kim, Y.X. Mejia, L.P. Lee, Nanophotonic crescent moon structures with sharp edge for ultrasensitive biomolecular detection by local electromagnetic field enhancement effect, Nano Lett. 5 (2005) 119–124, http://dx.doi.org/10.1021/nl048232+.
[5] J. Pérez-Juste, I. Pastoriza-Santos, L.M. Liz-Marzán, P. Mulvaney, Gold nanorods: synthesis, characterization and applications, Coord. Chem. Rev. 249 (2005) 1870–1901, http://dx.doi.org/10.1016/j.ccr.2005.01.030.
[6] G. Duan, W. Cai, Y. Luo, Z. Li, Y. Li, Electrochemically induced flowerlike gold nanoarchitectures and their strong surface-enhanced Raman scattering effect, Appl. Phys. Lett. (2006), http://dx.doi.org/10.1063/1.2392822.
[7] X. Ji, X. Song, J. Li, Y. Bai, W. Yang, X. Peng, Size control of gold nanocrystals in citrate reduction: the third role of citrate, J. Am. Chem. Soc. 129 (2007) 13939–13948, http://dx.doi.org/10.1021/ja074447k.
[8] J. Sharma, Y. Tai, T. Imae, Synthesis of confeito-Like gold nanostructures by a solution phase galvanic reaction, J. Phys. Chem. C 112 (2008) 17033–17037, http://dx.doi.org/10.1021/jp8053247.
[9] A.R. Tao, S. Habas, P. Yang, Shape control of colloidal metal nanocrystals, Small 4 (2008) 310–325, http://dx.doi.org/10.1002/smll.200701295.
[10] J. Sharma, T. Imae, Recent advances in fabrication of anisotropic metallic nanostructures, J. Nanosci. Nanotechnol. 9 (2009) 19–40.
[11] M. Brust, M. Walker, D. Bethell, D.J. Schiffrin, R. Whyman, Synthesis of thiol-derivatised gold nanoparticles in a two-phase liquid–liquid system, J. Chem. Soc. Chem. Commun. (1994) 801–802, http://dx.doi.org/10.1039/C39940000801.
[12] A. Manna, T. Imae, K. Aoi, M. Okazaki, Gold nanoparticles surface-confined by hybrid self-assembled monolayers of dendrimer and dodecanethiol, Mol. Simul. 29 (2003) 661–665, http://dx.doi.org/10.1080/0892702031000103202.
[13] K. Mitamura, T. Imae, N. Saito, O. Takai, Fabrication and self-assembly of hydrophobic gold nanorods, J. Phys. Chem. B 111 (2007) 8891–8898, http://dx.doi.org/10.1021/jp072524s.
[14] M. Osawa, K.-I. Ataka, K. Yoshii, Y. Nishikawa, Surface-enhanced infrared spectroscopy: the origin of the absorption enhancement and band selection rule in the infrared spectra of molecules adsorbed on fine metal particles, Appl. Spectrosc. 47 (1993) 1497–1502.
[15] T. Imae, H. Torii, In situ investigation of molecular adsorption on Au surface by surface-enhanced infrared absorption spectroscopy, J. Phys. Chem. B 104 (2000) 9218–9224, http://dx.doi.org/10.1021/jp001592a.
[16] M. Ujihara, N.M. Dang, C.-C. Chang, T. Imae, Surface-enhanced infrared absorption spectra of eicosanoic acid on confeito-like Au nanoparticle, J. Taiwan Inst. Chem. Eng. 45 (2014) 3085–3089, http://dx.doi.org/10.1016/j.jtice.2014.06.021.
[17] K. Yoshida, T. Itoh, V. Biju, M. Ishikawa, Y. Ozaki, Experimental evaluation of the twofold electromagnetic enhancement theory of surface-enhanced resonance Raman scattering, Phys. Rev. B 79 (2009) 085419, http://dx.doi.org/10.1103/PhysRevB.79.085419.

[18] C.-C. Chang, T. Imae, L.-Y. Chen, M. Ujihara, Efficient surface enhanced Raman scattering on confeito-like gold nanoparticle-adsorbed self-assembled monolayers, Phys. Chem. Chem. Phys. 17 (2015) 32328–32334, http://dx.doi.org/10.1039/C5CP05490G.
[19] S.S. Krupka, B. Wiltschi, U. Reuning, K. Hölscher, M. Hara, E.-K. Sinner, In vivo detection of membrane protein expression using surface plasmon enhanced fluorescence spectroscopy (SPFS), Biosens. Bioelectron. 22 (2006) 260–267, http://dx.doi.org/10.1016/j.bios.2006.01.004.
[20] F. Tam, G.P. Goodrich, B.R. Johnson, N.J. Halas, Plasmonic enhancement of molecular fluorescence, Nano Lett. 7 (2007) 496–501, http://dx.doi.org/10.1021/nl062901x.
[21] K. Mitamura, T. Imae, S. Tian, W. Knoll, Surface plasmon fluorescence investigation of energy-transfer-controllable organic thin films, Langmuir 24 (2008) 2266–2270, http://dx.doi.org/10.1021/la703001y.
[22] T. Imae, X. Zhang, Effect of Au nanorod assemblies on surface-enhanced Raman spectroscopy, J. Taiwan Inst. Chem. Eng. 45 (2014) 3081–3084, http://dx.doi.org/10.1016/j.jtice.2014.06.012.
[23] J. Paczesny, K. Sozański, I. Dzięcielewski, A. Żywociński, R. Hołyst, Formation of net-like patterns of gold nanoparticles in liquid crystal matrix at the air-water interface, J. Nanopart. Res. 14 (2012), http://dx.doi.org/10.1007/s11051-012-0826-4.
[24] S. Chen, Langmuir monolayers of gold nanoparticles: from ohmic to rectifying charge transfer, Anal. Chim. Acta 496 (2003) 29–37, http://dx.doi.org/10.1016/S0003-2670(03)00987-5.
[25] A. Swami, A. Kumar, P. Selvakannan, S. Mandal, M. Sastry, Langmuir–Blodgett films of laurylamine-modified hydrophobic gold nanoparticles organized at the air–water interface, J. Colloid Interface Sci. 260 (2003) 367–373, http://dx.doi.org/10.1016/S0021-9797(03)00047-X.
[26] S. Paul, C. Pearson, A. Molloy, M.A. Cousins, M. Green, S. Kolliopoulou, P. Dimitrakis, P. Normand, D. Tsoukalas, M.C. Petty, Langmuir-Blodgett film deposition of metallic nanoparticles and their application to electronic memory structures, Nano Lett. 3 (2003) 533–536, http://dx.doi.org/10.1021/nl034008t.
[27] K.L. Genson, J. Holzmueller, C. Jiang, J. Xu, J.D. Gibson, E.R. Zubarev, V.V. Tsukruk, Langmuir-Blodgett monolayers of gold nanoparticles with amphiphilic shells from V-Shaped binary polymer arms, Langmuir 22 (2006) 7011–7015, http://dx.doi.org/10.1021/la061163p.
[28] M. Ujihara, K. Mitamura, N. Torikai, T. Imae, Fabrication of metal nanoparticle monolayers on amphiphilic poly(amido amine) dendrimer langmuir films, Langmuir 22 (2006) 3656–3661, http://dx.doi.org/10.1021/la053202n.
[29] Z. Matharu, P. Pandey, M.K. Pandey, V. Gupta, B.D. Malhotra, Functionalized gold nanoparticles –Octadecylamine hybrid langmuir-Blodgett film for enzyme sensor, Electroanalysis 21 (2009) 1587–1596, http://dx.doi.org/10.1002/elan.200904578.
[30] P. Pienpinijtham, X. Xia Han, S. Ekgasit, Y. Ozaki, An ionic surfactant –mediated Langmuir–Blodgett method to construct gold nanoparticle films for surface-enhanced Raman scattering, Phys. Chem. Chem. Phys. 14 (2012) 10132–10139, http://dx.doi.org/10.1039/C2CP41419H.
[31] H.M. Osorio, P. Cea, L.M. Ballesteros, I. Gascón, S. Marqués-González, R.J. Nichols, F. Pérez-Murano, P.J. Low, S. Martín, Preparation of nascent molecular electronic devices from gold nanoparticles and terminal alkyne functionalised monolayer films, J. Mater. Chem. C 2 (2014) 7348–7355, http://dx.doi.org/10.1039/C4TC01080A.
[32] F. Le, D.W. Brandl, Y.A. Urzhumov, H. Wang, J. Kundu, N.J. Halas, J. Aizpurua, P. Nordlander, Metallic nanoparticle arrays: a common substrate for both surface-Enhanced raman scattering and surface-enhanced infrared absorption, ACS Nano 2 (2008) 707–718, http://dx.doi.org/10.1021/nn800047e.
[33] X. Zhang, T. Imae, Perpendicular superlattice growth of hydrophobic gold nanorods on patterned silicon substrates via evaporation-Induced self-assembling, J. Phys. Chem. C 113 (2009) 5947–5951, http://dx.doi.org/10.1021/jp808864v.
[34] E. Fülöp, N. Nagy, A. Deák, I. Bársony, Langmuir–Blodgett films of gold/silica core/shell nanorods, Thin Solid Films 520 (2012) 7002–7005, http://dx.doi.org/10.1016/j.tsf.2012.07.097.
[35] E. Gergely-Fülöp, N. Nagy, A. Deák, Langmuir-Blodgett films of gold nanorods with different silica shell thicknesses, Periodica Polytechnica Chem. Eng. 59 (2015) 104–110, http://dx.doi.org/10.3311/PPch.7596.
[36] M. Ujihara, T. Imae, Versatile one-pot synthesis of confeito-like Au nanoparticles and their surface-enhanced Raman scattering effect, Coll. Surf. A 436 (2013) 380–385, http://dx.doi.org/10.1016/j.colsurfa.2013.07.003.
[37] F.H. Ho, Y.-H. Wu, M. Ujihara, T. Imae, A solution-based nano-plasmonic sensing technique by using gold nanorods, Analyst 137 (2012) 2545–2548, http://dx.doi.org/10.1039/C2AN35101C.
[38] K. Mitamura, T. Imae, N. Saito, O. Takai, Surface modification of gold nanorods by organosilanes, Compos. Interfaces 16 (2009) 377–385, http://dx.doi.org/10.1163/156855409X447138.
[39] O. Mori, T. Imae, Atomic force microscope observation of monolayers of arachidic acid, octadecyldimethylamine oxide, and their mixtures, Langmuir 11 (1995) 4779–4784, http://dx.doi.org/10.1021/la00012a032.
[40] A. Manna, T. Imae, M. Iida, N. Hisamatsu, Formation of silver nanoparticles from a N-hexadecylethylenediamine silver nitrate complex, Langmuir 17 (2001) 6000–6004, http://dx.doi.org/10.1021/la010389j.
[41] H. Song, F. Kim, S. Connor, G.A. Somorjai, P. Yang, Pt nanocrystals: shape control and Langmuir-Blodgett monolayer formation, J. Phys. Chem. B 109 (2005) 188–193, http://dx.doi.org/10.1021/jp0464775.
[42] B. Nikoobakht, Z.L. Wang, M.A. El-Sayed, Self-assembly of gold nanorods, J. Phys. Chem. B 104 (2000) 8635–8640, http://dx.doi.org/10.1021/jp001287p.
[43] A. Brioude, X.C. Jiang, M.P. Pileni, Optical properties of gold nanorods: DDA simulations supported by experiments, J. Phys. Chem. B 109 (2005) 13138–13142, http://dx.doi.org/10.1021/jp0507288.
[44] P.K. Jain, K.S. Lee, I.H. El-Sayed, M.A. El-Sayed, Calculated absorption and scattering properties of gold nanoparticles of different size, shape, and composition: applications in biological imaging and biomedicine, J. Phys. Chem. B 110 (2006) 7238–7248, http://dx.doi.org/10.1021/jp057170o.
[45] S. Eustis, M.A. El-Sayed, Why gold nanoparticles are more precious than pretty gold: noble metal surface plasmon resonance and its enhancement of the radiative and nonradiative properties of nanocrystals of different shapes, Chem. Soc. Rev. 35 (2006) 209–217, http://dx.doi.org/10.1039/B514191E.
[46] S.K. Ghosh, T. Pal, Interparticle coupling effect on the surface plasmon resonance of gold nanoparticles: from theory to applications, Chem. Rev. 107 (2007) 4797–4862, http://dx.doi.org/10.1021/cr0680282.
[47] P.K. Jain, S. Eustis, M.A. El-Sayed, Plasmon coupling in nanorod assemblies: optical absorption, discrete dipole approximation simulation, and exciton-coupling model, J. Phys. Chem. B 110 (2006) 18243–18253, http://dx.doi.org/10.1021/jp063879z.
[48] S.A. Maier, H.A. Atwater, Plasmonics: localization and guiding of electromagnetic energy in metal/dielectric structures, J. Appl. Phys. (2005), http://dx.doi.org/10.1063/1.1951057 10.1021/cr0680282ccc.